

SHEAR AND BOND DETERIORATION IN BEAM-COLUMN JOINTS  
UNDER BIDIRECTIONAL LOAD REVERSALS

S. T. Burguières, Jr.,<sup>I</sup> J. E. Longwell,<sup>II</sup> and J. O. Jirsa<sup>III</sup>

SUMMARY

An experimental program on the behavior of interior reinforced concrete beam-column joints under bidirectional load reversals is described. Of particular interest is the influence of shear and bond deterioration of the concrete in the joint on the reduction of stiffness and strength of the test specimen.

INTRODUCTION

Little experimental work has been reported on the behavior of reinforced concrete frames under bidirectional seismic loads. Current design procedures [1,2] are based on analysis and proportioning of the frame considering that the seismic excitation coincides with the axes of planar frames which make up the structural system. However, during a major earthquake, large deformations and yielding of the structural system may occur simultaneously in both directions. In an earlier paper [3], the influence of different loading histories on the response of three identical specimens was reported. The tests showed that the shear capacity of the joint remained nearly constant under (a) unidirectional loading in one direction, no racking loads in orthogonal direction, Specimen 1-U-C; (b) alternate bidirectional loading, racking loads applied in only one direction at a time, Specimen 3-BA-C; and (c) bidirectional simultaneous, racking loads applied to both beam directions simultaneously so that the resultant load and deflection coincided with a diagonal axis through the joint, Specimen 2-BS-C. The objective of this report is to examine the behavior of four specimens subjected to bidirectional simultaneous loading in which the beam longitudinal steel and joint transverse steel was varied.

DESCRIPTION OF TESTS

The test specimen geometry is shown in Fig. 1. The specimen represents an interior beam-column joint of a frame without a slab. Beam details and reinforcing are shown in Fig. 1 and Table 1. Since these tests were intended to demonstrate joint distress, the specimen was designed so that joint strength and stiffness would be critical in influencing

---

<sup>I</sup>Graduate Research Assistant, Department of Civil Engineering, The University of Texas at Austin, Austin, Texas 78712.

<sup>II</sup>Graduate Research Assistant, Department of Civil Engineering, The University of Texas at Austin, Austin, Texas 78712.

<sup>III</sup>Professor of Civil Engineering, The University of Texas at Austin, Austin, Texas 78712.

subassembly behavior. High joint shear, reinforcing bar bond conditions, and minimal confining reinforcement in the joint were intentionally considered in design to ensure that these problems could be observed.

Nominal design material strengths were 28 MPa for the concrete and 420 MPa for the reinforcing steel. Actual values are listed in Table 1. Column reinforcing and axial load in the column were selected so that full beam yielding could occur before column yielding. This was done to meet current seismic design recommendations, which follow the weak beam-strong column frame design philosophy. Note that in each specimen the beams had the same main reinforcing in both directions, but that bars were displaced vertically as necessary to pass through the joint region.

Specimens were fabricated in the upright position, with the first casting completing the lower column, the beams and the joint region, and the bottom 15 cm of the upper column. A second casting completed the remainder of the upper column.

A sketch of the idealized loading of an interior beam-column joint subassembly is shown in Fig. 2. No attempt was made to exactly duplicate all the aspects of loading and restraint in a concrete-framed structure subjected to seismic loading.

Figure 3 shows a specimen situated in the loading apparatus. Specimens were tested in the upright position, braced against a floor-wall reaction system. Four vertical rods and centerhole rams applied column axial load. Four rams with spherical end attachments, attached to the reaction floor, loaded the beam stubs up or down. The upper column was effectively pin-supported at the top and braced to the reaction wall to resist upper column shear. The bottom of the lower column was semi-rigidly connected to the reaction floor. An inflection point formed a short distance above this connection to match approximately the idealized loading condition shown in Fig. 2.

Axial load applied to the column was held at a constant level of 1335 kN compression during all four tests. This value was equal to the balance load for the column for bending in one direction only. Racking loads were applied to the beam pairs, with deformation of the beam ends controlled. In order to simulate the effects of dead load on the subassembly, all four beams were deformed downward 2.5 mm before beginning cyclic deformations. Cycling of beam deformation was performed about the "dead load" deflection which cracked the beams. The loading pattern for the north and west beams is shown in Fig. 4. The south and east beams would be identical except for direction of load. Load cycles are numbered for reference in subsequent figures.

All measurements of load, deformation, and reinforcing bar strain were made by a computer-controlled data acquisition unit. The computer link permitted interactive data reduction as the testing progressed.

#### BEHAVIOR

The results will be described briefly using resultant beam moment-interstory drift relationships determined in the tests. The resultant beam

moment is the total racking moment (applied beam load times distance from column center to point of loading) applied to the subassemblage about the center of the joint. The racking moment is computed for the NS and EW axes and the resultant along a 45° diagonal is computed. The interstory displacements are computed from measured beam end displacements in the NS and EW direction using a rigid body rotation to produce zero beam end deflection. The resulting horizontal displacement at the end of the column is equivalent to the interstory drift for a subassembly in a frame except that eccentricity ( $P-\Delta$ ) of axial load is not included in the test.

2-BS-C. This specimen had a high beam moment capacity. Figure 5 shows that the beam moments applied to the specimen were well below the calculated beam or column flexural capacity. In the second cycle at  $2\Delta$ , the specimen exhibited considerable degradation of strength and stiffness. It is likely that the joint shear capacity was reached in this specimen. Bond deterioration was expected to be high because large bars were used; however, it should be noted that the beams may not have reached yield.

4-BS-B. Figure 6 shows that the beam moments reached calculated yield moment. The specimen had only 2/3 of the beam longitudinal reinforcement used in 2-BS-C. The second and third cycles of load at each deflection level showed considerable degradation of load and stiffness, probably due to shear distress in the joint and loss of anchorage through the joint due to yielding and slip of the bar.

5-BS-A. The specimen was identical to 4-BS-B except that the size and number of beam bars were changed to alter the bond characteristics of the bars without changing the flexural strength of the beams. As can be seen by comparing Figs. 6 and 7, very little difference in response was observed. Figure 9 shows 5-BS-A after testing. The cracking and spalling in the joint region is typical of all four specimens tested. Figure 10 shows the bar stress in a #8 top bar in 5-BS-A plotted against beam end deflection. The stresses were determined from strains measured about 20 cm from the column face. It is interesting to note that the strains attempt to go into compression as the beam is loaded upward initially; however, compression is never realized and at load point 3 (see Fig. 4) substantial tension has developed. With downward loading, tension increases and the bar yields. The measured strains indicate that bond was destroyed along the bar through the joint and steel normally considered to be in compression was in tension throughout the loading history.

7-BS-D. This specimen is identical to 5-BS-A, except that the transverse reinforcement in the joint was increased by a factor of 5. Figure 8 shows that the response was nearly the same as 4-BS-B and 5-BS-A. The only discernible difference is a slightly higher moment at the first cycle peaks to new deflection levels. Because the joint confinement was increased in 7-BS-D, it was felt that the joint shear distress would be decreased. Using instrumentation developed to measure joint shear strains, it was possible to determine the resultant joint shear (from a free body of the joint) and to plot a joint shear vs shear strain for the test specimens (Figs. 11 and 12). The magnitude of shear strain from peak to peak is nearly the same in both axes; however, the deformations for 7-BS-D tended to be symmetrical about the axis. The shape of the curves is also nearly identical.

(2) Bond deterioration along bars through the joint occurs very early in the load history and, combined with shear distress, produces a severe reduction in energy absorbing capacity. Only limited improvement in the bond deterioration problem was realized when smaller bars were used.

(3) The strength and stiffness characteristics of the four joints tested were approximately the same. The joint shear deformations were not influenced by changes in beam or joint reinforcement. However, the inelastic deformations attributed to the columns and beams showed significant changes as the transverse reinforcement was increased and as the beams reached flexural yield.

#### ACKNOWLEDGMENT

The support of the National Science Foundation through Grants ENV75-00192 and ENV77-20816 for this work is gratefully acknowledged. The opinions, findings, and conclusions are those of the authors and do not necessarily reflect the views of the National Science Foundation.

#### REFERENCES

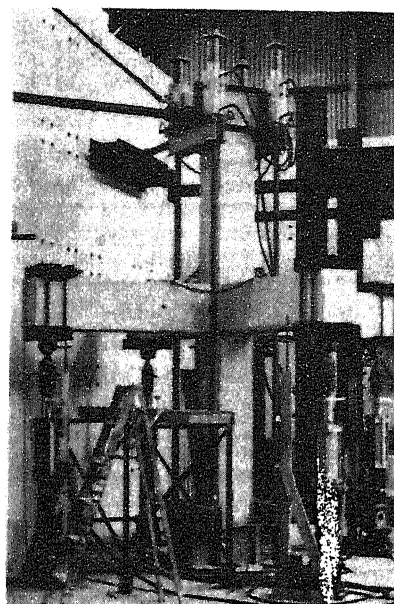
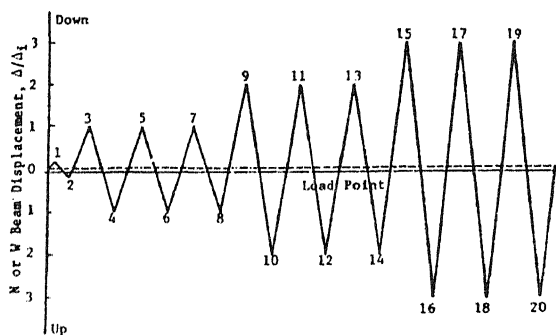
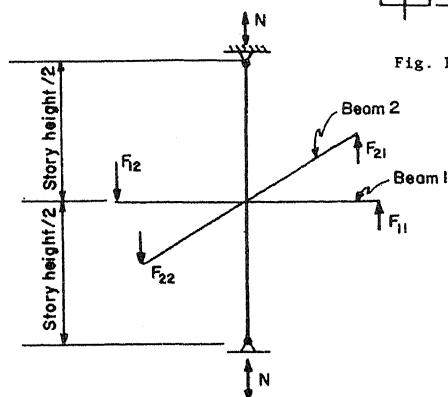
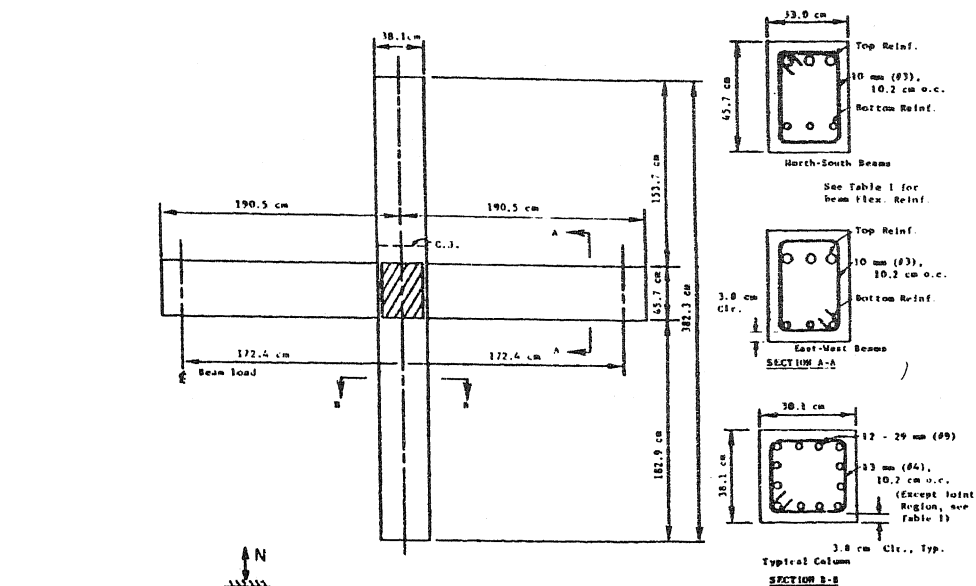
1. Meinheit, D. F., and Jirsa, J. O., "The Shear Strength of Reinforced Concrete Beam-Column Joints," CESRL Report No. 77-1, The University of Texas at Austin, January 1977.
2. ACI-ASCE Committee 352, "Recommendations for Design of Beam-Column Joints in Monolithic Reinforced Concrete Structures," Journal of the American Concrete Institute, Proc. V. 73, No. 7, July 1976.
3. Burguières, S. T., Jr., Jirsa, J. O., and Longwell, J. E., "The Behavior of Beam-Column Joints under Bidirectional Load Reversals," CEB Symposium, Rome, 1979.

TABLE 1 TEST SPECIMENS

| Specimen | $f'_c$<br>MPa | Beam Reinforcement |             |           |             | Joint Reinforcement |             | Maximum<br>Resultant<br>Joint<br>Shear,<br>MPa |
|----------|---------------|--------------------|-------------|-----------|-------------|---------------------|-------------|--|
|          |               | Top                |             | Bottom    |             |                     |             |  |
|          |               | Size, mm           | $f_y$ , MPa | Size, mm  | $f_y$ , MPa | Size; Spacing<br>mm | $f_y$ , MPa |  |
| 2-B3-C   | 28.1          | 3-#10 (32)         | 500         | 3-#8 (25) | 426         | #4 (13)@127*        | 440         | 2740   |
| 4-B3-C   | 28.4          | 2-#10 (32)         | 500         | 2-#8      | 426         | #4 (13)@127*        | 440         | 2420   |
| 5-B3-A   | 30.4          | 3-#8 (25)          | 426         | 3-#6 (19) | 435         | #4 (13)@127*        | 440         | 2190   |
| 7-B3-D   | 33.2          | 3-#8 (25)          | 426         | 3-#6 (19) | 435         | #4 (13)@ 64**       | 440         | 2260   |

\*One closed hoop at each spacing.

\*\*Two closed hoops at each spacing.



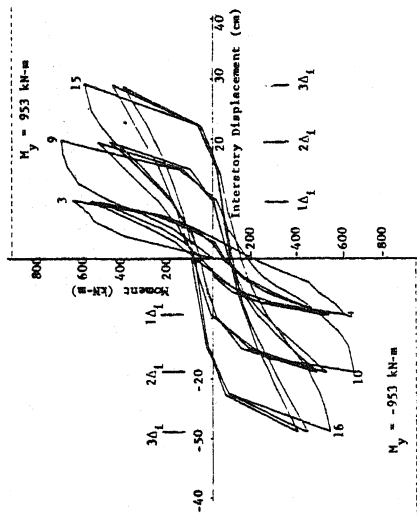


Fig. 5 Total Beam Moment vs Iterative Displacement (2-B5-C)

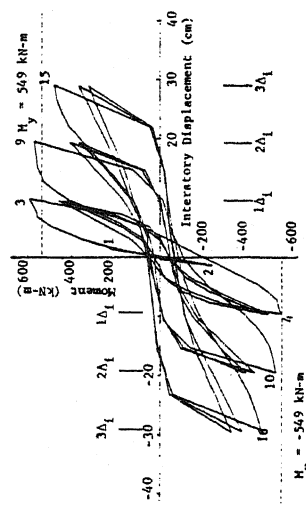


Fig. 7 Total Beam Moment vs Iterative Displacement (5-B5-A)

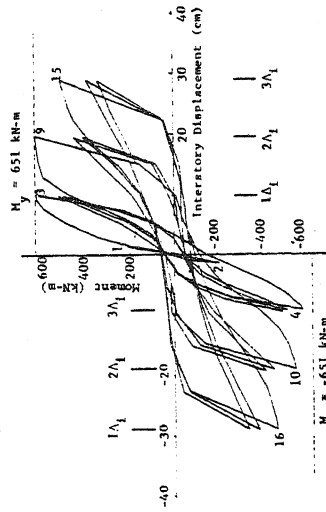


Fig. 6 Total Beam Moment vs Iterative Displacement (4-B5-B)

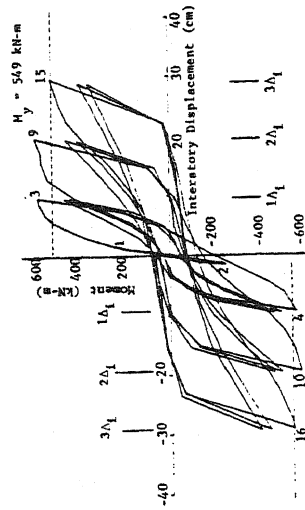


Fig. 8 Total Beam Moment vs Iterative Displacement (7-B5-D)

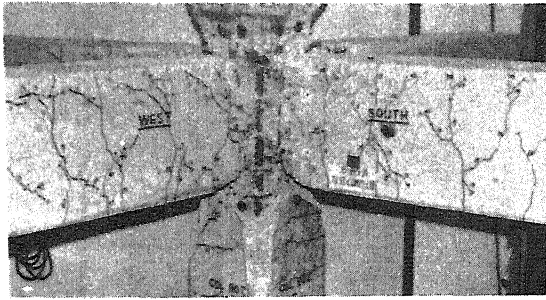


Fig. 9 Specimen 5-BS-A After Testing

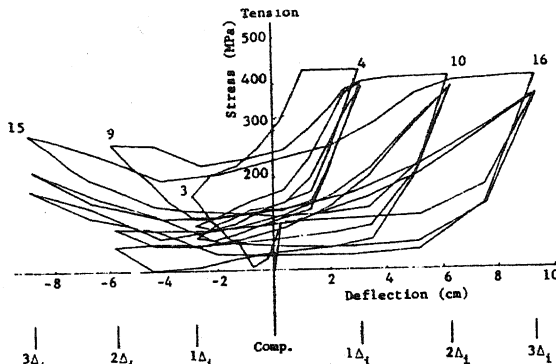


Fig. 10 #8 Top Bar Stress vs Beam Deflection (5-BS-A)

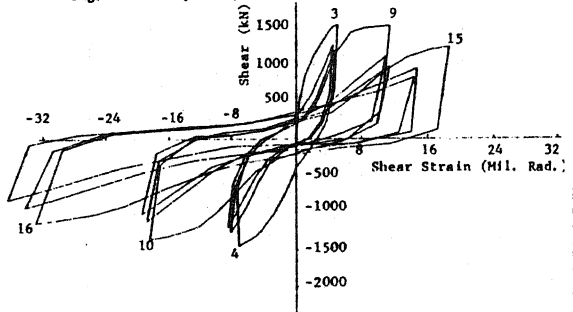


Fig. 11 Joint Shear vs Joint Shear Strain (4-BS-B)

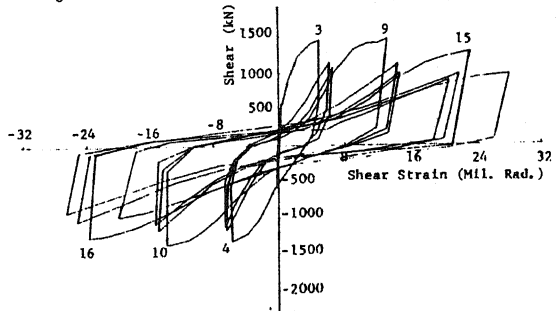


Fig. 12 Joint Shear vs Joint Shear Strain (7-BS-D)

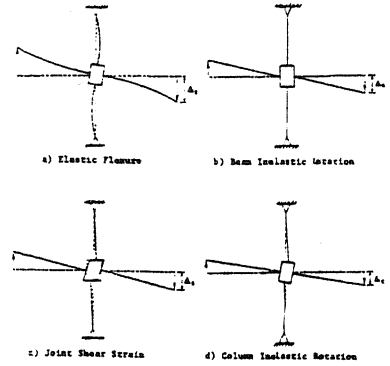


Fig. 13 Components of Beam Displacement

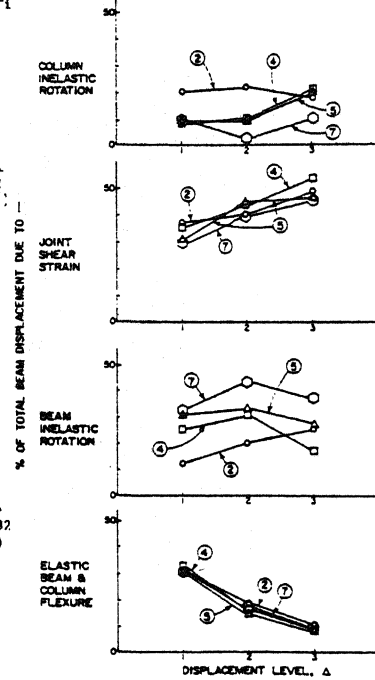


Fig. 14 Percentages of Component Displacements